Post-print of: Zhikun Xu, et al. “Targeting low-density lipoprotein receptors with protein-only nanoparticles” in Journal of nanoparticle research (Springer), Vol. 17 issue 3 (March 2015) , article 150. The final versión is available at DOI: 10.1007/s11051-015-2959-8

Targeting low density lipoprotein receptors with protein-only nanoparticles.

Zhikun Xu [1, 2, 3], María Virtudes Céspedes [3, 4], Ugutz Unzueta [1, 2, 3], Patricia Álamo [3, 4], Mireia Pesarrodona [1, 2, 3], Ramón Mangues [3, 4], Esther Vazquez [1, 2, 3], Antonio Villaverde [1, 2, 3 *], Neus Ferrer-Miralles [1, 2, 3 *]

[1] Institut de Biotecnologia i de Biomedicina, Universitat Autònoma de Barcelona, Bellaterra, 08193 Barcelona, Spain
[2] Departament de Genètica i de Microbiologia, Universitat Autònoma de Barcelona, Bellaterra, 08193 Barcelona, Spain
[3] CIBER de Bioingeniería, Biomateriales y Nanomedicina (CIBER-BBN), Bellaterra, 08193 Barcelona, Spain
[4] Oncogenesis and Antitumor Drug Group, Biomedical Research Institute Sant Pau (IIB-SantPau), Hospital de la Santa Creu i Sant Pau, C/ Sant Antoni Maria Claret, 167, 08025 Barcelona, Spain

Contact:

NFM Email: neus.ferrer@uab.cat; phone : +34935812148 ; fax : +34 5812011

AV Email: antoni.villaverde@uab.cat; phone +34935813086 ; fax : +34 5812011

Abstract

Low density lipoprotein receptors (LDLR) are appealing cell surface targets in drug delivery, as they are expressed in the blood-brain barrier (BBB) endothelium and are able to mediate transcytosis of functionalized drugs for molecular therapies of the central nervous system (CNS). On the other hand, brain-targeted drug delivery is currently limited, among others, by the poor availability of biocompatible vehicles, as most of the nanoparticles under development as drug carriers pose severe toxicity issues. In this context, protein nanoparticles offer functional versatility, easy and cost-effective bioproduction and full biocompatibility. In this study, we have designed and characterized several chimerical proteins containing different LDLR ligands, regarding their ability to bind and internalize target cells and to self-organize as viral mimetic agents. While the self-assembling of LDLR-binding proteins as nanoparticles positively influences cell penetration *in vitro*, the nano-particulate architecture might be not favouring BBB crossing *in vivo*. These findings are discussed in the context of the use of nanostructured materials as vehicles for the systemic treatment of CNS diseases.

Keywords: Recombinant protein; self-assembling; nanoparticles, LDLR; cell targeting; BBB

Introduction

Cell-targeted drug delivery and personalized medicines strongly push towards the development of biocompatible materials adapted to deliver cargo drugs to specific cell types. A critical point in such design process is the selection of intrinsically non-toxic materials, which while keeping high structural and functional tunability would not induce side effects upon administration. Because of their biodegradability, biocompatibility and functional and structural plasticity, proteins are highly convenient materials to construct carriers for the delivery of both conventional and emerging drugs (Lohcharoenkal et al., 2014). On the other hand, drug vehicles, apart from exhibiting powerful targeting properties, should overcome the sequential biological barriers encountered previous to reaching the right cell compartment in the target organ. This is compulsory when targeting the central nervous system (CNS) that is protected by the blood-brain barrier (BBB) and by the blood spinal cord barrier. Since in a therapeutic context, local administration into brain is not desirable because its invasiveness (Lockman et al., 2002), systemic administration is mandatory and empowering drugs to cross the BBB has become a major issue in current pharmacology and nanomedicine (Pardridge, 2010). BBB tightly controls the access of molecules and drugs to brain, either by paracelullar or transcellular pathways, by using both functional and structural elements addressed to maintain brain homeostasis (Barbu et al., 2009). Hydrophilic and cationic small molecules show some spontaneous penetrability. However, usual chemical drugs and therapeutic proteins cannot cross the BBB or are targets for the efflux pumps acting in the BBB. A nanoparticulate organization of vehicles used for systemic drug delivery increases drug stability and circulation time (Cespedes et al., 2014), what preventing renal filtration offers potential for sustained release of the cargo. Although these and other properties of nanostructured materials are highly desirable, paracelullar penetration of nanoparticles targeted to the central nervous system (CNS) is assumed to be especially problematical. Functionalization with ligands of hormone receptors or transporters for transcytosis is then mandatory despite the unexpected BBB-crossing activities exhibited by a few polymers used for nanoparticle fabrication and coating (eg polysorbate 80 and poly-[ethylene glycol-co-hexadecyl]-cyanoacrylate (Kim et al., 2007; Kreuter et al., 2002a)).

A catalogue of potential BBB-crossing peptides and proteins for functionalization is available (Van et al., 2012) (http://brainpeps.ugent.be). Among them, ligands binding transferrin, insulin and low density lipoprotein receptors (LDLR) have been especially appealing because of their transcytotic properties. LDLR, in particular, are of additional

interest as they are overexpresed in several human conditions including lung, stomach and cervical cancers. Several LDRL protein ligands, namely ApoB (Spencer and Verma, 2007b); ApoE (Re et al., 2011; Wagner et al., 2012) and Apo A-I (Fioravanti et al., 2012; Kratzer et al., 2007), have been already used to functionalize diverse types of drugs and nanoparticles to allow or enhance BBB crossing. Others, such as Kunitz-derived peptides (Angiopeps), presented in plain protein-drug complexes, have entered clinical trials addressed to brain tumors. (Kurzrock et al., 2012). (http://clinicaltrials.gov/ct2/show/NCT01480583?term=ANG1005&rank=6). Although several of these LDLR ligands have proved to be promising, the ideal architecture for the drug-ligand complex to effectively cross the BBB and reach the brain remains to be elucidated. In particular, whether the ligand would be more effective when functionalizing a nanostructured vehicle than when applied in plain ligand-drug complexes remains unsolved, being a critical issue that needs further investigation (Juillerat-Jeanneret, 2008).

In the present study we have selected several known peptidic LDLR ligands and explored them as BBB crossers, in protein-only materials under several presentations. Some of these constructs self-organize as nanoparticulate materials while others remain in monomeric, unassembled forms. The *in vitro* and *in vivo* analyses of cell penetrability, biodistribution and brain targeting provide new concepts about the BBB crossing properties of functional protein nanoparticles, and suggest divergent diffusion properties when acting in cell culture and upon systemic administration.

Materials and methods

Protein production and purification

Vectors derived from pET-22a and harboring *angiopep-2-GFP-H6*, *seq-1-GFP-H6* and *apoB-GFP-H6* gene sequences had been designed in-house and constructed by Genscript. These plasmids were transformed into *Escherichia coli* BL21 (DE3) and positive clones selected in presence of 100 µg/ml ampicillin. Transformed bacteria were cultured in 750 ml LB (Luria Bertani, Conda Cat. 1551.00) medium in presence of 100 µg/ml ampicillin at 37 °C until OD_{550}=0.5, and incubated further overnight at 28 °C with 1 mM isopropyl β-D-1-thiogalactopyranoside (IPTG) to trigger protein production. Bacteria were harvested through centrifugation and resuspended in Tris buffer (20 mM Tris-HCl pH 8.0, 500 mM NaCl, 10 mM Imidazol) in the presence of EDTA-free protease inhibitor (Complete EDTA-Free; Roche).Then, cells were disrupted by a French press (Thermo FA-078A) at 1100 psi, and the soluble fraction separated from the mixture by centrifugation at 15,000 g for 30 min. The insoluble fraction from ApoB-GFP-H6 was stored at -80°C for further use.

All proteins were purified by His affinity chromatography in an ÄKTA purifier FPLC (GE healthcare). After filtering the soluble fraction, samples were loaded onto HiTrap Chelating HP 1 ml columns (GE healthcare), washed with Tris wash buffer (20 mM Tris-HCl pH 8.0, 500 mM NaCl, 10 mM Imidazol) and eluted with Tris elution buffer (20 mM Tris-HCl pH 8.0, 500 mM NaCl, 500 mM Imidazol). After purification, corresponding fractions were collected and then dialyzed against carbonate buffer (166 mM $NaHCO_3$, pH 7.4) overnight at 4°C. Proteins were characterized by mass spectrometry and quantified by Bradford assay. Some of these activities were technically supported by the Protein Production Platform CIBER-BBN/UAB (http://www.ciber-bbn.es/en/programas/89-plataforma-de-produccion-de-proteinas-ppp).

Protein purification from inclusion bodies

The pellet of ApoB-GFP-H6 IBs was washed with water twice, and resuspended with solubilizing buffer (40 mM Tris with 0.2 % N-lauroyl sacosine, pH 8.0) in a ratio 1:40 and incubated for 24 h at room temperature. After that, the sample was centrifuged at 15000 g for 30 min. Resuspended soluble protein from IBs was purified as described above with prior N-lauroyl sarcosine removal by using a Hitrap QFF ion exchange column (GE healthcare).

Cell culture and flow cytometry

HeLa (ATCC-CCL-2) cells were cultured in DMEM (GIBCO, Rockville, MD) supplemented with 10 % Fetal Calf Serum (GIBCO) at 37 °C and 5 % CO_2. Human umbilical vein endothelial cells (HUVEC) were maintained in M199 (Invitrogen) with 5 % Fetal Calf Serum (FBS) and 1.2 mM L-Glutamine, at 37 °C. Cells were incubated with recombinant proteins (1 μM and 9 μM) for 24 h and further treated with 1 mg/ml trypsin for 15 min to remove non-internalized protein. Then cells were collected and analyzed on a FACSCanto system (Becton Dickinson), using a 15 W air-cooled argon-ion laser at 488 nm excitation. GFP fluorescence emission was measured with detector D (530/30 nm band pass filter). In endosomal escape of proteins experiment, chloroquine was added 4 h before adding protein to the cell, and reach a final concentration of 100 μM, after that, cells were incubated with chloroquine and recombinant protein for 24 h, and then treated with the same procedure.

Transmission electron microscopy (TEM)

Purified proteins were diluted to 0.2 mg/ml in dialysis buffer (166 mM $NaHCO_3$, pH 7.4), deposited onto carbon-coated grids for 2 min, stained with uranyl acetate and observed in a Hitachi H-7000 transmission electron microscope.

Confocal microscopy

HeLa cells were seeded on Mat-Teck culture dishes (Mat Teck Corp., Ashland, MA, USA), and after 24 h, 2 μM of protein was added to cell culture, then it was incubated for another 24 h. The nucleus was stained with Hoechst 33342 (0.2 μg/ml, Molecular Probes) and plasma membrane was stained with CellMask™ Deep Red (2.5 μg/ml, Molecular Probes) for 5 min in darkness. Later, cells were washed with PBS (Sigma-Aldrich Chemie GmbH, Steinheim, Germany). Stained cells were examined using TCS-SP5 confocal laser scanning microscope (Leica Microsystems, Heidelberg, Germany) with a Plan Apo 63×/1.4 (oil HC × PL APO l blue) objective. Hoechst 33342 was excited by a blue diode (405 nm) and detected at the 415-460 nm range. GFP proteins were excited by an Ar laser (488 nm) and detected at the 525-545 nm range. CellMask was excited by a HeNe laser (633 nm) and detected at the 650-775 nm range. Z-series were collected at 0.5 μm intervals.

Fluorescence determination and dynamic light scattering (DLS)

All proteins were diluted to 400 μg/ml; then GFP fluorescence was determined by Cary Eclipse Fluorescence Spectrophotometer (Variant) at detection wavelength of 510 nm,

by using an excitation wavelength of 450 nm. Volume size distribution of nanoparticles and monomeric GFP fusions were determined by dynamic light scattering at 633 nm (Zetasizer Nano ZS, Malvern Instruments Limited, Malvern, UK).

Cell permeability analysis

Permeability studies were performed at the USEF Drug Screening Platform (http://www.usc.es/en/investigacion/riaidt/usef). Briefly, CaCo2 cells were cultured in DMEM high in glucose supplemented with 10 % FBS, 1 % nonessential amino acids (100x), 1 % L-glutamine, 100 U/ml penicillin, 100 µg/ml streptomycin 95 % air and 5 % CO_2 and at 37 °C. The cells (CaCo2, passage 65) were seeded in the apical compartment of a sterile 6-well transwell at a density of 250,000 cells / well in 1.5 ml of medium and 2.5 ml of fresh medium was then added to the basal compartment. Cells were maintained in this medium for 21 days until complete differentiation (renewing the medium every 2 days). After this time, the medium was changed to HBSS (0.9 mM $CaCl_2$, 0.5 mM $MgCl_2$, and 20 mM HEPES, pH 7.4).

Transepithelial resistance (TEER) measurement was conducted using a Millipore epithelial voltmeter (Millicell-ERS) in a 6 well traswell (Costar). After adding HBSS in both compartments, samples were added in the apical part at different time intervals (0, 30, 60 sec and 20 min) for TEER measurements. To determine protein transport through Caco2, the amount of transported protein was determined by the measurements of fluorescence in basal compartment over time. Experiments were performed in triplicate. Data were expressed as % of initial TEER. The % is calculated based on the formula: % Initial TEER = (TO / TI) * 100; where TO is the TEER observed in the wells with the samples under study and TI is the TEER observed before addition of samples. The transport was assessed by the apparent permeability (cm / sec), the amount is represented as protein against time and the slope of the linear fit (Δamount /Δtime) was used to calculate the apparent permeability (Papp) by the formula: Papp = (Δamount / Δtime) / (AxC_0); where A is the area of the growth surface (4.71 cm^2) and C_0 is the initial concentration (µM) present in the apical compartment.

***In vivo* model and biodistribution analyses**

Five-week-old female Swiss nu/nu mice weighing between 18 and 20 g (Charles River, L-Abreslle, France) and maintained in SPF conditions, were used for *in vivo* studies. All the *in vivo* procedures were approved by the Hospital de Sant Pau Animal Ethics Committee and performed according to EC directives. Proteins were injected

intravenously at a dose of 500 µg/mouse (n=3 mice), control mice was injected with $NaHCO_3$ buffer. At 5, 15, 30 min, 1 h and 2 h after injection, mice were anesthetized with isofluorane and whole body fluorescence was monitored using IVIS spectrum equipment (Xenogen, France). After that, mice were sacrificed and brain, kidney, lung and liver collected and examined separately at 30 min and 2 h for GFP fluorescence in an IVIS Spectrum. The *ex vivo* fluorescent recording of the brain was performed sequentially, first measuring the emission from whole brain and then of sagittal sections to achieve a complete fluorescent signal characterization.

Statistical analyses

Data were analyzed using one-way ANOVA and post hoc Tukey tests.

Results

Three chimerical genes were constructed to produce LDLR-binding recombinant proteins (Table 1), based on the following modular organization; from N- to C-termini, ligand, linker, EGFP and H6 tail (Figure 1A). Such organization had been previously proved useful in promoting the spontaneous formation of highly stable fluorescent protein nanoparticles, provided a sufficient positive electrostatic charge is present at the N terminus of the whole fusion (Cespedes et al., 2014; Unzueta et al., 2012). Angiopep-2 and Seq-1 fusions were produced in *E. coli* as fully soluble versions while ApoB-GFP-H6 obtained from the soluble cell fraction was partially proteolized. In fact, protein sequencing by Edman degradation procedure of the soluble protein form revealed loss of the amino-terminal 34-mer peptide of ApoB (Table 1) in approximately 50 % of the protein population (not shown). Then, since the LDLR ligand was lost in this protein fraction the concentration of this construct was adjusted in further experiments to manage a comparative amount of full-length protein. However, in the insoluble cell fraction, the full length ApoB-GFP-H6 was detected as a unique protein band (Figure 1B). Mass spectrometry analysis demonstrated that the insoluble protein version showed the predicted molecular mass corresponding to the intact construct. *In vitro* refolding of ApoB-GFP-H6 IBs rendered homogeneous soluble protein preparations.

Table 1. Amino acid sequences of protein ligands and known or putative targets.

Ligand	**Aa sequence**	**Target**	**References**
Angiopep-2	TFFYGGSRGKRNNFKTEEY	VLDLR	(Demeule et al., 2008)
Seq-1	KYLAYPDSVHIW	N/A	(Maggie, 2011)
ApoB	SSVIDALQYKLEGTTRLTRKRGLKLA TALSLSNK**F**VEGS	LDLR	(Spencer and Verma, 2007a)

VLDLR: Very-low-density-lipoprotein receptor

N/A: Not available but a LDLR family member

LDLR: Low density lipoprotein receptor

Bold amino acid letter: first amino acid detected in the short ApoB form in the soluble cell fraction

In a preliminary screening (Unzueta et al., 2012), Angiopep-2 and Seq-1 were observed as unable to promote the assembling of the fusion proteins in higher order

nanoparticles, probably due to their low cationic amino acid content, although doubts remained about the potential influence of the composition of the different buffers used to store the proteins. All the proteins produced here were tested again for nanoparticle formation under homogeneous buffer conditions as described above, in 166 mM $NaHCO_3$, pH 7.4. The exclusive occurrence of unassembled forms of Seq-1-GFP-H6 and Angiopep-2-GFP-H6 was indeed confirmed (Figure 2A), with a particle size, determined by DLS, compatible with that of GFP monomers or dimers (as GFP naturally tends to dimerization). Contrarily, ApoB-GFP-H6 formed nanoparticles in both its natural soluble form directly obtained from recombinant bacteria (ApoB-GFP-H6s), or when refolded *in vitro* from IBs (ApoB-GFP-H6IBs) (Figure 2A). However, ApoB-GFP-H6s nanoparticles appeared to be unstable, as they peaked at 28 nm but also over 100 nm, indicative of aggregation. ApoB-GFP-H6IBs nanoparticles, instead, showed a unique monodisperse peak at 18 nm (Figure 2A), compatible with the formation of robust supramolecular structures. The aggregation of ApoB-GFP-H6s suspected in DLS measures was clearly confirmed by TEM, since amorphous protein clusters abounded in the fields (Figure 2B). This was in contrast with the highly regular architecture observed in 18 nm-ApoB-GFP-H6IBs particles (Figure 2B). Interestingly, all recombinant proteins retained GFP fluorescence (Figure 2C), with only moderate reduction in the case of Angiopep-2-GFP-H6 and ApoB-GFP-H6IBs. Importantly, the preservation of fluorescence emission allowed further characterization of the constructs' biological properties by fluorescence analysis and imaging.

In this regard, we first wanted to explore cell penetrability of all constructs in cells displaying and not displaying LDLRs. Uptake of protein constructs in $LDLR^-$ HUVEC was indeed negligible when comparing with that of closely related nanoparticles empowered by the unspecific but highly efficient cell penetrating peptide R9 (nine sequential arginines, (Vazquez et al., 2010)) (Figure 3A). In contrast, penetrability was highly stimulated in $LDLR^+$ HeLa cells (Figure 3B), especially in the case of ApoB-GFP-H6IBs. In presence of chloroquine, internalization of ApoB-GFP-H6IBs protein in HeLa cell population dramatically increased (Figure 4), indicative of an endosomal route as expected for any receptor-mediated uptake (Vazquez et al., 2008). Interestingly, the penetrability of ApoB-GFP-H6s was always lower than that of ApoB-GFP-H6IBs. This fact suggests that an unstable nanoparticle might be less suitable for proper receptor binding and cell internalization. Alternatively, the folding status of the protein (probably different as derived from the soluble cell fraction or from refolding) might influence ligand exposure and/or particle performance in a biologically significant way. The efficient cell penetration of ApoB-GFP-H6IBs was fully confirmed by confocal

microscopy (Figure 5). In general, the unassembled constructs were internalized by cells in a less efficient way, and the uptake was not influenced by background protein precipitation in the extracellular medium that has been generally observed in GFP-based self-assembling proteins (Vazquez et al., 2010).

Considering these cell internalization results, the transepithelial crossing efficiency of the LDLR-ligand functionalized modular proteins was determined in a fully stablished *in vitro* BBB model based on CaCo2 cells (Hellinger et al 2012) (Table 2). In the two protein concentrations tested, ApoB-GFP-H6IBs presented the highest penetrability in accordance with the internalization assays presented above (Figure 3). Angiopep-2-GFP-H6 and Seq-1-GFP-H6 also displayed minor but still important penetrability in this BBB model at high protein concentration, thus suggesting a potential to effectively cross the BBB. However, when ApoB-GFP-H6s was challenged to the CaCo2 cell barrier, the apparent permeability was even lower than the negative control GFP, again indicating a failure of these protein nanoparticles to reach a fully functional status. Indeed, the stability of the Caco2 cell monolayer is shown in the data related to Papp of one the protein constructs (ApoB-GFP-H6s) at both protein concentrations maintained low through the experiment.

Table 2. *In vitro* transepithelial crossing activity of BBB-targeted GFP proteins

Protein	**Concentration (μM)**	**Papp (cm/s)x10^{-6}**
Angiopep-2-GFP-H6	2	0.41±0.006
	10	16.6±1.5
Seq-1-GFP-H6	2	2.58±0.18
	10	9.75±0.004
ApoB-GFP-H6s	2	0.21±0.09
	10	0.79±0.09
ApoB-GFP-H6IBs	2	12.46±1.03
	10	18.02±4.79
GFP	2	0.69±0.08
	10	2.41±0.44

In a step further, and particularly encouraged by the good performance of ApoB-GFP-H6IBs nanoparticles we wanted to examine the biodistribution of the protein set and the

potential influence of the supramolecular protein organization, upon systemic administration through the tail vein in healthy mice in which side events that affect brain permeability such as enhanced permeability and retention (EPR) effect do not take place. We were specifically interested in this issue as at one side, LDLR are important targets in BBB-crossing for drug delivery into the CNS (Demeule et al., 2008; Kim et al., 2007; Spencer and Verma, 2007b), and also, cationic protein nanoparticles are biocompatible materials that fulfil most of the requests posed for vehicle-mediated drug delivery into brain (Juillerat-Jeanneret, 2008). Therefore, we analysed *ex vivo* the signal from the whole brain to avoid the noise coming form the background of the whole body imaging followed by ex vivo recording of brain sagittal sections to complete evaluation of the extent of the emitted fluorescence. The analyses of these samples clearly indicated BBB-crossing properties of Angiopep-2-GFP-H6 and Seq-1-GFP-H6 (Figure 6A). Angiopep-2-GFP-H6, in particular, was observed as accummulating in the brain parenchyma 30 min after administration, a fact that was fully assesed by quantitative analysis of fluorescence under conditions that not allowed GFP-H6 background signal (Figure 6B,C). Surprisingly, ApoB-GFP-H6s but also ApoB-GFP-H6IBs failed to accummulate into brain (Figure 6), indicating that the ApoB ligand was unable to drive the crossing of BBB under the presentation offered by the resulting nanoparticles.

To understand better the stability in circulation and the potential renal clearance of both BBB-crossing and failing constructs, GFP fluorescence was also determined in kidney. All the constructs that did not form nanoparticles (namely Angiopep-2-GFP-H6 and Seq-1-GFP-H6, and the parental GFP-H6) and also the unstable ApoB-GFP-H6s nanoparticles accummulated in kidney (Figure 7A, B), indicative of renal clearance and consequently, of a material size under 8 nm (Cespedes et al., 2014). This is in agreement with the unability of Angiopep-2-GFP-H6 and Seq-1-GFP-H6 to self-assemble, and it also suggests that the ApoB-GFP-H6s nanoparticles, observed *in vivo* as unstable, probably dissasamble once in the bloodstream (maybe due to the high salt content of the biological fluid). No fluorescence was recorded in lung and liver, in any case (not shown).

These data indicates that a nanoparticulated architecture of ligand-containing proteins, promoting efficient cell penetrability and transcytosis, is neither sufficient nor necessary to reach the brain under systemic administration, and that unassembled soluble proteins, even when undergoing an effective renal clearance, are able to cross the BBB in a significant fraction.

Discussion

Proteins are excellent functional carriers for therapeutic nucleic acids and conventional drugs (Aris and Villaverde, 2004; Nehate et al., 2014). When fused to the amino terminus of a His tagged GFP, the cationic peptide ApoB promotes the formation of nanoparticles that are only composed by the modular protein acting as self-interacting building block. This is based on a recently proposed protein engineering principle that allows designing protein nanoparticles by the fusion of cationic peptides to polyhistidine tagged polypeptides, and that act irrespective of the nature and sequence of the core protein (Cespedes et al., 2014; Unzueta et al., 2012). Nanoparticle formation is promoted by the hydrostatic contacts between the resulting dipolar monomers, but the whole supramolecular structure is largely stabilized by additional forces such as Van der Waals, hydrogen bond interactions (Cespedes et al., 2014; Unzueta et al., 2014), and protein-DNA interactions if used as non-viral gene therapy vehicle (Unzueta et al., 2014). Interestingly, the amino terminal cationic peptide (ApoB in case of the current study) acts as an architectonic tag but also as a LDLR ligand with known BBB-crossing properties (see Table 1). Under the same conditions, the less cationic Seq-1 and Angiopep-2 peptides, also LDLR ligands, fail in promoting nanoparticle formation (Figure 2).

On the other hand, ApoB-GFP-H6 nanoparticles have been obtained from two alternative protein sources, namely the soluble *E. coli* cell fraction (ApoB-GFP-H6s) or by *in vitro* refolding of purified ApoB-GFP-H6 IBs (ApoB-GFP-H6IBs). Although both protein versions act as self-organizing building blocks (Figure 2), ApoB-GFP-H6s nanoparticles are poorly stable as determined by DLS and by TEM (Figure 2). Then, the protein was found in kidney soon upon administration (Figure 7). Renal clearance was also observed in the parental GFP-H6 and in the unassembled Seq-1-GFP-H6 and Angiopep-2-GFP-H6 (Figure 7). In contrast, the robust ApoB-GFP-H6IBs particles with a regular size of 18 nm were not cleared by kidney, what necessarily results in a prolonged and stable circulation of the protein in the bloodstream. The time extended occurrence of ApoB-GFP-H6s in kidney 2 h after administration, not observed in any strictly monomeric protein (namely GFP-H6, Seg-1-GFP-H6 and Angiopep-2-GFP-H6, Figure 7), could be indicative of a progressive disassembling of the nanoparticles once in the bloodstream, and of a dynamic balance between assembled and disassembled forms. This would favor again the hypothesis of the intrinsic architectonic instability of ApoB-GFP-H6s particles. The differences in the stability of ApoB-GFP-H6IBs and ApoB-GFP-H6s, and also the differential cell penetrability of these constructs (Figure 3B, 4, 5), can be only attributed to different conformations of the protein as resulting

from either the soluble cell fraction or from refolding from protein aggregates. For instance, the ApoB tail in ApoB-GFP-H6s might be more involved in crossmolecular contacts between building blocks and less available for cellular interactions. Of course, the heterogeneity in protein bands detected in the Western blot analysis of the soluble *E. coli* cell fraction, probably resulting from selective proteolysis (Figure 1B), could also contribute to this fact. Therefore, the conformational and structural status of protein building blocks of *de novo* designed nanoparticles, and the influence of the cell factory in the quality and properties of the final supramolecular assemblies is a currently neglected field that deserves deeper exploration (Ferrer-Miralles et al., 2013). This is especially relevant in the context of emerging biomaterials resulting from *in vivo* fabrication (Vazquez and Villaverde, 2013), the rising number of conventional and non-conventional cell factories for protein and polymer production (Corchero et al., 2013; Ferrer-Miralles and Villaverde, 2013) and the new bio-engineering strategies to improve microbial biosynthesis regarding industrial and biopharma applications (Chen, 2012; Lee et al., 2012; Rodriguez-Carmona and Villaverde, 2010).

On the other hand, ApoB-GFP-H6IBs nanoparticles internalized cultured cells more efficiently than ApoB-GFP-H6s nanoparticle versions and than Seq-1-GFP-H6 and Angiopep-2-GFP-H6 proteins (Figure 3B, 5). The penetration of ApoB-GFP-H6IBs took place, as expected, in $LDLR^+$ cells but not in $LDLR^-$ cells (Figure 3A). The control R9-GFP-H6 nanoparticles, which are empowered by a potent Tat-inspired unspecific cell penetrating peptide (R9), do not shown any LDLR-linked preference in internalization (Figure 3). LDLR-dependent internalization is dramatically enhanced by chloroquine (Figure 4), indicative of an endosomal pathway. Under these conditions, ApoB-GFP-H6IBs but no other constructs was essentially found in all cells among the population exposed to the nanoparticle, even when applied at moderate doses (1 µM).

Although based on the good performance in *in vitro* experiments, ApoB-GFP-H6IBs particles were highly promising regarding BBB-crossing, none ApoB-derived protein version was found in the brain parenchyma up to two hours after iv administration (Figure 6). Surprisingly, Seq-1-GFP-H6 and Angiopep-2-GFP-H6 proteins were detected in brain in *ex vivo* imaging, with an occurrence that peaked at around 30 min. BBB-crossing of these two proteins occurred even with important renal filtration (Figure 7), while skipping renal clearance did not promoted, by itself, brain localization of ApoB-derivatives. Being ApoB a well-known BBB-crossing peptide for soluble drugs (Kreuter et al., 2002b) and also when linked to nanoparticles (Kim et al., 2007), failure in a proper activity when empowering protein nanoparticles might be due to

inappropriate presentation of the ligand in these kind of constructs. In fact, due to its cationic nature, ApoB acts as both architectonic and targeting agent with limited solvent exposure when compared to ligands in monomeric proteins. Although such a dual activity is not by itself an obstacle for proper biodistribution of protein nanoparticles (as exemplified by the peptide T22 in similar GFP-based constructs) (Cespedes et al., 2014; Unzueta et al., 2012) and also for ligand-mediated cell penetrability (Figure 3 and 4), the most complex biological barriers imposed by brain vessels might represent a tighter bottleneck to proper biodistribution.

Conclusions

The results presented here upon exploration of three recombinant protein-only LDLR ligands, presented in a total of four versions, reveal that high cellular penetrability in cultured cells does not guarantee efficient BBB-crossing and brain targeting mediated by transcytosis-associated receptors. Interestingly, protein versions in form of nanoparticles do penetrate cultured cells more efficiently than unassembled constructs, while the contrary is true regarding *in vivo* BBB-crossing. Such a divergent performance prompts to evaluate the use of nanoparticulate materials for BBB-crossing therapies, which even being highly efficient in cell culture might find *in vivo* bottlenecks essentially distinguishable from those encountered when aiming to targets other than brain.

LEGENDS

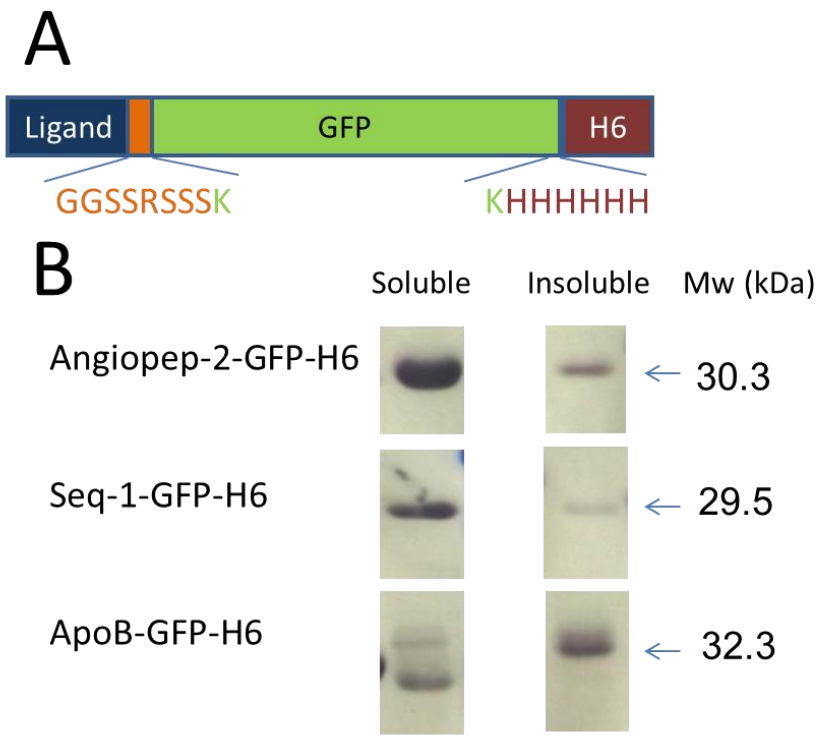

Figure 1. Structure of the fusion proteins. A) EGFP was used as the core of the fusions (green), flanked by a cell ligand at the N-terminus (blue) and a hexahistidine at the C-terminus (brown). A linker segment (orange) was placed between the ligand and GFP. Residues in green indicate the end terminal amino acids of GFP in the joining regions. The sequences of the fused N-terminal ligands are depicted in Table 1. B) Western blot analyses of disrupted bacteria producing the different fusion proteins, upon fractioning.

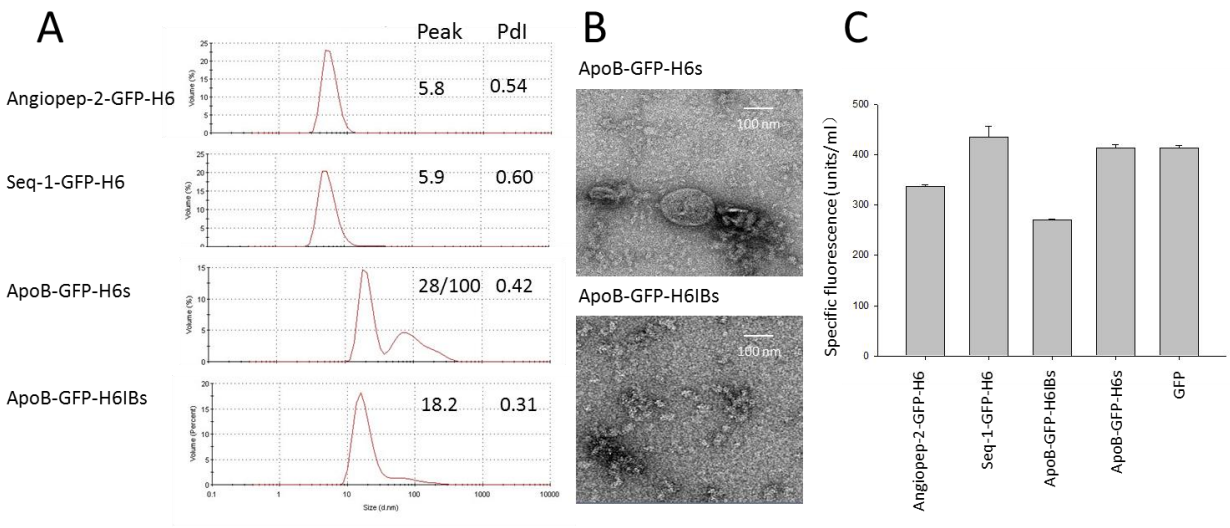

Figure 2. Characterization of proteins and protein nanoparticles. A) Size distribution of purified proteins, determined by DLS. Pdi is polydispersion index. B) TEM analyses of two versions of ApoB-GFP-H6, namely straightforward soluble protein or protein species refolded from IBs. C) Specific fluorescence emission of all protein versions, compared to that of commercial, control GFP.

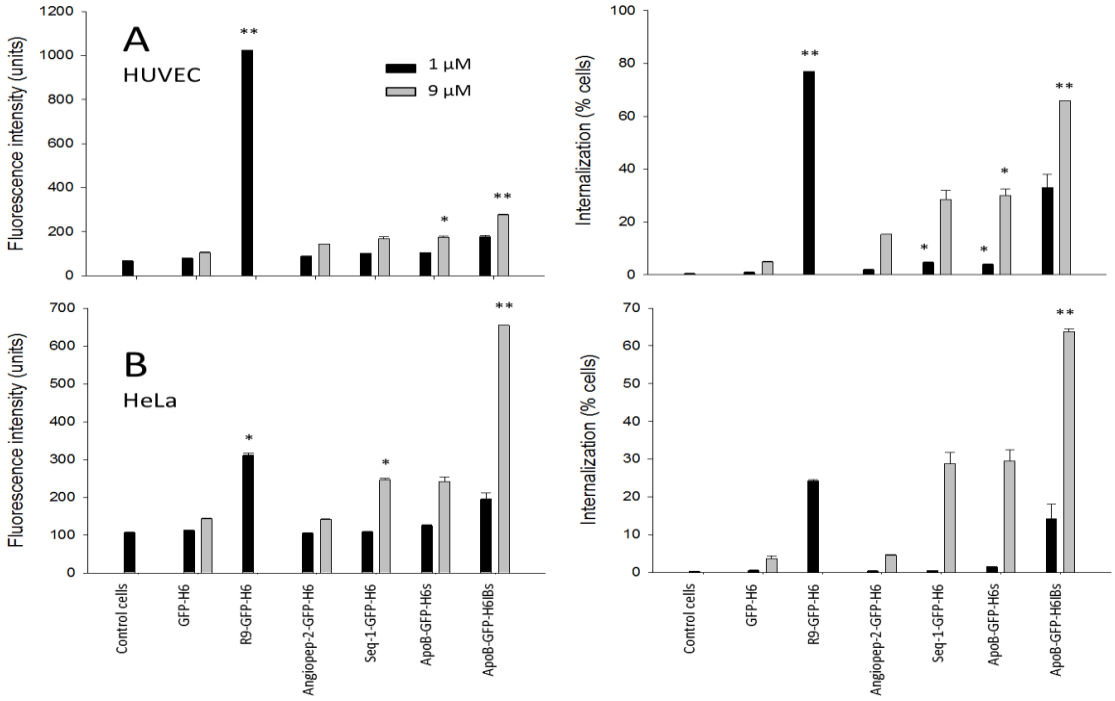

Figure 3. Internalization of proteins and protein nanoparticles. Cell penetrability was determined by both total fluorescence emission (left) and by the fraction of fluorescent cells (right). Targets were LDLR$^-$ HUVEC (A) and LDLR$^+$ HeLa (B) cells. Proteins were added to the cultures at two alterative concentrations, namely 1 and 9 µM. Those proteins showing significant differences with GFP-H6 are labelled with asterisks (**, p<0.01; *, p<0.05).

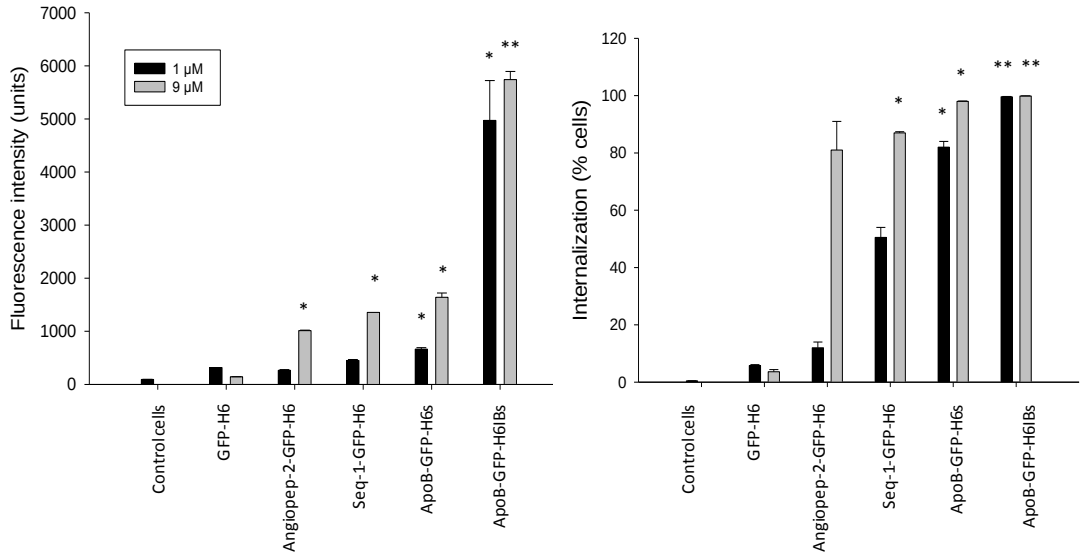

480

Figure 4. Endosomal escape of proteins and protein nanoparticles. Cell penetrability was determined by both total fluorescence emission (left) and by the fraction of fluorescent cells (right). Data have been obtained in LDLR^{+} HeLa cells in presence of
485 chloroquine. Those proteins showing significant differences with GFP-H6 are labelled with asterisks (**, p<0.01; *, p<0.05). Note the differences in the Y scale when comparing to Figure 3.

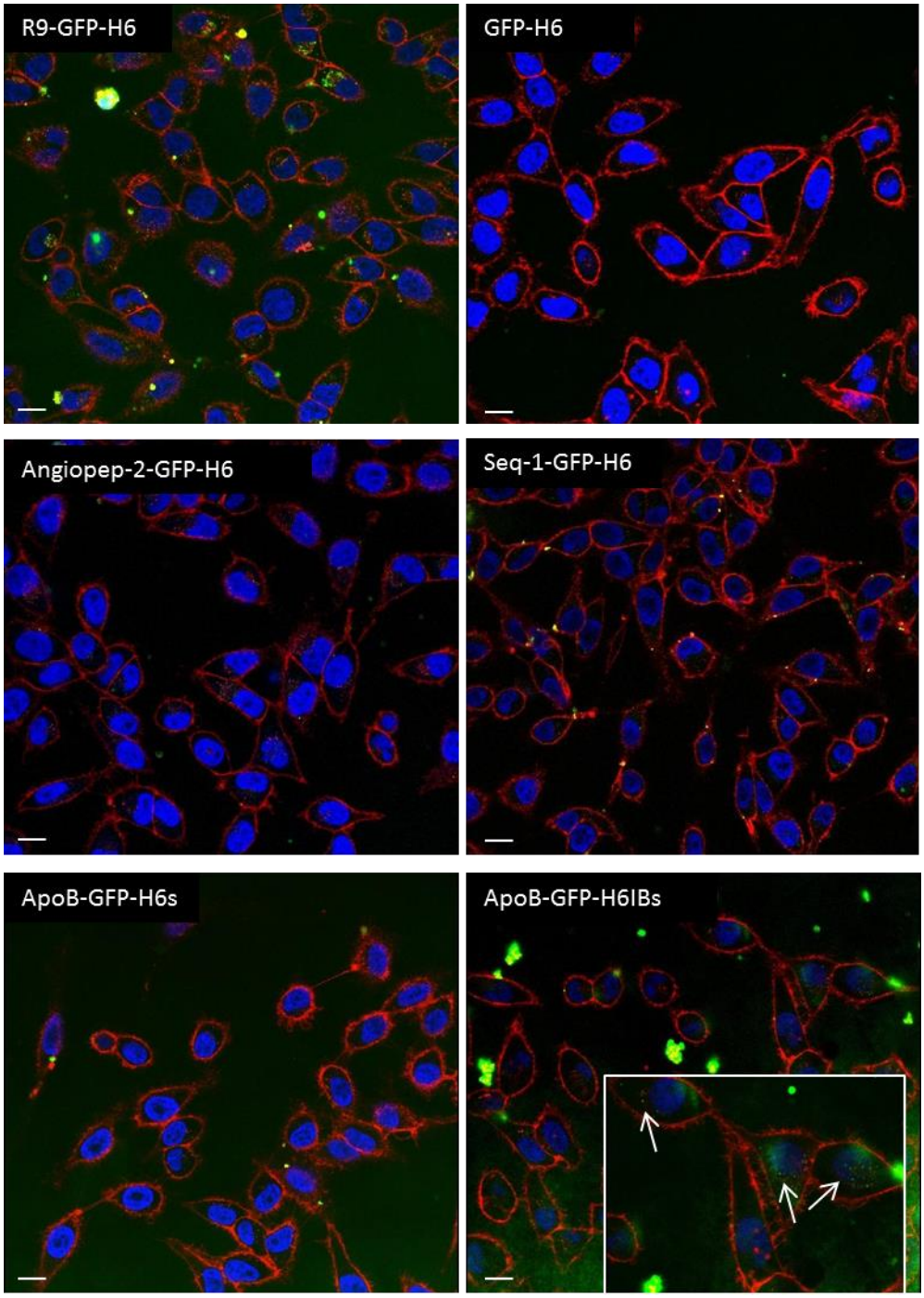

Figure 5. Internalization of proteins and protein nanoparticles monitored by confocal microscopy in HeLa cells. The white bars indicate 15 µm. A magnified inset of ApoB-GFP-H6IBs has been included to stress the nanoparticulate nature of the internalized material (arrows), despite some extracellular protein precipitation. Nuclei are labeled in blue and cell membranes in red.

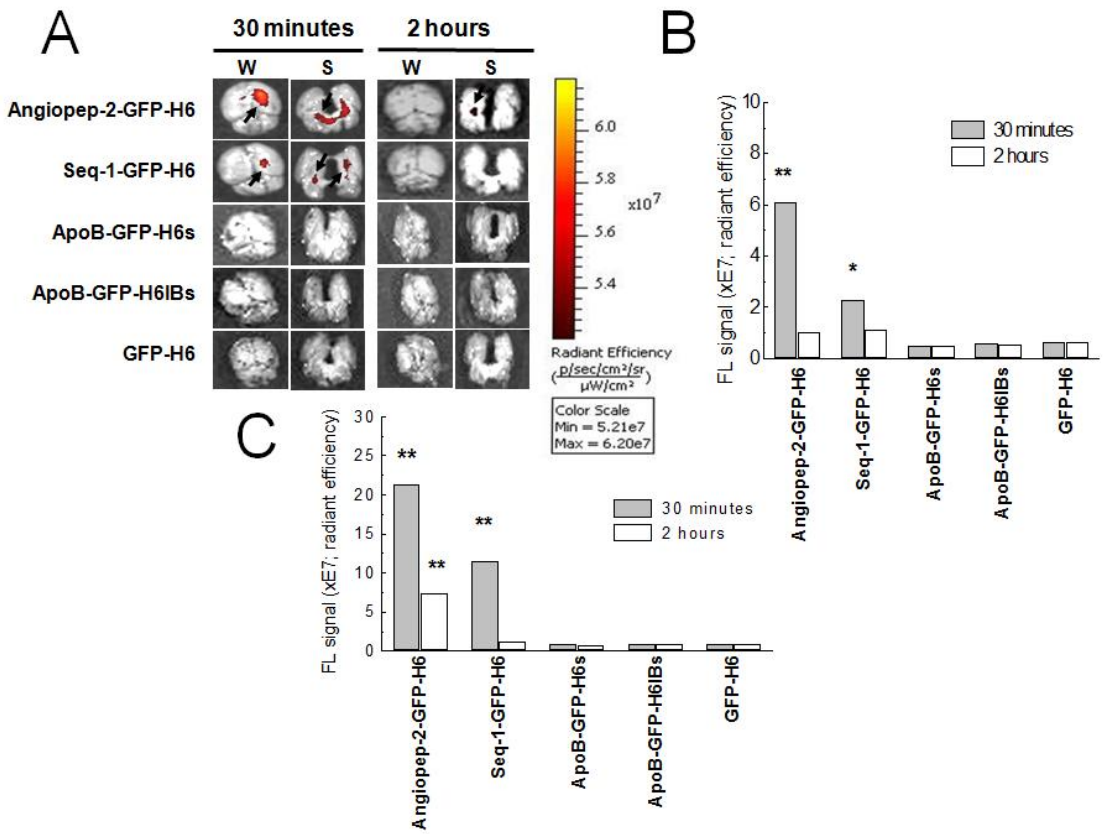

Figure 6. Biodistribution of proteins and protein nanoparticles in *ex vivo* imaging. GFP fluorescence registered *ex vivo* in mouse whole brain (*W*) and sagittal sections (*S*) at 30 minutes and 2 hours after iv administration of 500 µg of each protein. Black arrows show fluorescence signal accumulation in the brain parenchyma (A). Quantitative determination of GFP fluorescence analyzed in whole brain (B) and sagittal sections (C) expressed as the total radiant efficiency (photon/s/cm2/sr/µW/cm2). Those proteins showing significant differences with the rest of proteins are labelled with asterisks (**, $p<0.01$; *, $p<0.05$). Data from 30 min and 2 h samples have been compared separately.

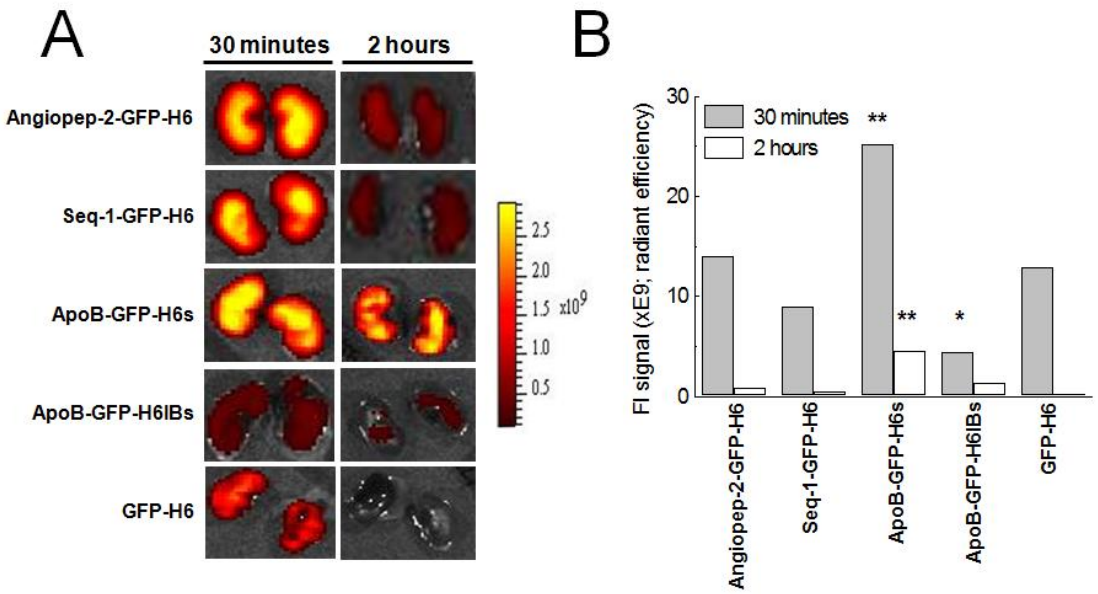

Figure 7. Renal clearance of protein nanoparticles in *ex vivo* imaging. GFP fluorescence registered *ex vivo* in mouse kidneys 30 minutes and 2 hours after iv administration of 500 µg of each construct (A). Quantitative determination of GFP fluorescence expressed as the total radiant efficiency (photon/s/cm2/sr/µW/cm2) (B). Those proteins showing significant differences with the rest of proteins are labelled with asterisks (**, $p<0.01$; *, $p<0.05$). Data from 30 min and 2 h samples have been compared separately.

Acknowledgments: We are grateful to the Protein Production Platform (CIBER-BBN - UAB) for helpful technical assistance and for protein production and purification services (http://www.ciber-bbn.es/en/programas/89-plataforma-de-produccion-de-proteinas-ppp). We are indebted to FIS PI12/01861, Marató 416/C/2013-2030 and NanoMets to RM, MINECO BIO2013-41019-P to AV, AGAUR (2014SGR-132) and CIBER de Bioingeniería, Biomateriales y Nanomedicina (project NANOPROTHER) for funding our research on protein-based therapeutics. We thank the CIBER-BBN Nanotoxicology Unit for fluorescent in vivo follow-up using the IVIS equipment. We are also indebted to the Cell Culture and Citometry Units of the Servei de Cultius Cel·lulars, Producció d'Anticossos i Citometria (SCAC), and to the Servei de Microscòpia, both at the UAB, and to the Soft Materials Service (ICMAB-CSIC/CIBER-BBN). CIBER-BBN is an initiative funded by the VI National R&D&i Plan *2008-2011*, Iniciativa Ingenio 2010, Consolider Program, CIBER Actions and financed by the Instituto de Salud Carlos III with assistance from the European Regional Development Fund. Z.X. and M.P. acknowledge financial support from China Scholarship Council and Universitat Autònoma de Barcelona through pre-doctoral fellowships respectively. AV received an ICREA ACADEMIA award.

Reference List

Aris A, Villaverde A: Modular protein engineering for non-viral gene therapy. Trends Biotechnol 2004, 22: 371-377.

Barbu E, Molnar E, Tsibouklis J, Gorecki DC: The potential for nanoparticle-based drug delivery to the brain: overcoming the blood-brain barrier. Expert Opin Drug Deliv 2009, 6: 553-565.

Cespedes MV, Unzueta U, Tatkiewicz W, Sanchez-Chardi A, Conchillo-Sole O, Alamo P et al.: In Vivo Architectonic Stability of Fully de Novo Designed Protein-Only Nanoparticles. ACS Nano 2014.

Chen GQ: New challenges and opportunities for industrial biotechnology. Microb Cell Fact 2012, 11: 111.

Corchero JL, Gasser B, Resina D, Smith W, Parrilli E, Vazquez F et al.: Unconventional microbial systems for the cost-efficient production of high-quality protein therapeutics. Biotechnol Adv 2013, 31: 140-153.

Demeule M, Regina A, Che C, Poirier J, Nguyen T, Gabathuler R et al.: Identification and design of peptides as a new drug delivery system for the brain. J Pharmacol Exp Ther 2008, 324: 1064-1072.

Ferrer-Miralles N, Villaverde A: Bacterial cell factories for recombinant protein production; expanding the catalogue. Microb Cell Fact 2013, 12: 113.

Ferrer-Miralles N, Rodriguez-Carmona E, Corchero JL, Garcia-Fruitos E, Vazquez E, Villaverde A: Engineering protein self-assembling in protein-based nanomedicines for drug delivery and gene therapy. Crit Rev Biotechnol 2013, 10.3109/07388551.2013.833163 [doi].

Fioravanti J, Medina-Echeverz J, Ardaiz N, Gomar C, Parra-Guillen ZP, Prieto J et al.: The Fusion Protein of IFN-alpha and Apolipoprotein A-I Crosses the Blood-Brain Barrier by a Saturable Transport Mechanism. 2012, 188: 3988-3992.

Hellinger E, Veszelka S, Tóth AE, Walter F, Kittel A, Bakk ML, Tihanyi K, Háda V, Nakagawa S, Duy TD, Niwa M, Deli MA, Vastag M: Comparison of brain capillary endothelial cell-based and epithelial (MDCK-MDR1, Caco-2, and VB-Caco-2) cell-based surrogate blood-brain barrier penetration models.Eur J Pharm Biopharm. 2012, 82: 340-351

Juillerat-Jeanneret L: The targeted delivery of cancer drugs across the blood-brain barrier: chemical modifications of drugs or drug-nanoparticles? Drug Discov Today 2008, 13: 1099-1106.

Kratzer I, Wernig K, Panzenboeck U, Bernhart E, Reicher H, Wronski R et al.: Apolipoprotein A-I coating of protamine-oligonucleotide nanoparticles increases particle uptake and transcytosis in an in vitro model of the blood-brain barrier. 2007, 117: 301-311.

Kim HR, Andrieux K, Gil S, Taverna M, Chacun H, Desmaele D et al.: Translocation of poly(ethylene glycol-co-hexadecyl)cyanoacrylate nanoparticles into rat brain endothelial cells: role of apolipoproteins in receptor-mediated endocytosis. Biomacromolecules 2007, 8: 793-799.

Kreuter J, Shamenkov D, Petrov V, Ramge P, Cychutek K, Koch-Brandt C et al.: Apolipoprotein-mediated transport of nanoparticle-bound drugs across the blood-brain barrier. J Drug Target 2002, 10: 317-325.

Kurzrock R, Gabrail N, Chandhasin C, Moulder S, Smith C, Brenner A et al.: Safety, Pharmacokinetics, and Activity of GRN1005, a Novel Conjugate of Angiopep-2, a Peptide Facilitating Brain Penetration, and Paclitaxel, in Patients with Advanced Solid Tumors. 2012, 11: 308-316.

Lee SY, Mattanovich D, Villaverde A: Systems metabolic engineering, industrial biotechnology and microbial cell factories. Microb Cell Fact 2012, 11: 156.

Lockman PR, Mumper RJ, Khan MA, Allen DD: Nanoparticle technology for drug delivery across the blood-brain barrier. Drug Dev Ind Pharm 2002, 28: 1-13.

Maggie J.M.. Peptide for transmigration across blood brain barrier and delivery systems comprising the same. United States Patent Application Publication US 2011/0165079 A1. 2011.

Nehate C, Jain S, Saneja A, Khare V, Alam N, Dubey R et al.: Paclitaxel Formulations: Challenges and Novel Delivery Options. Curr Drug Deliv 2014.

Re F, Cambianica I, Sesana S, Salvati E, Cagnotto A, Salmona M et al.: Functionalization with ApoE-derived peptides enhances the interaction with brain capillary endothelial cells of nanoliposomes binding amyloid-beta peptide. 2011, 156: 341-346.

Rodriguez-Carmona E, Villaverde A: Nanostructured bacterial materials for innovative medicines. Trends Microbiol 2010, 18: 423-430.

Spencer BJ, Verma IM: Targeted delivery of proteins across the blood-brain barrier. Proc Natl Acad Sci U S A 2007, 104: 7594-7599.

Unzueta U, Ferrer-Miralles N, Cedano J, Zikung X, Pesarrodona M, Saccardo P et al.: Non-amyloidogenic peptide tags for the regulatable self-assembling of protein-only nanoparticles. Biomaterials 2012, 33: 8714-8722.

Unzueta U, Cespedes MV, Ferrer-Miralles N, Casanova I, Cedano JA, Corchero JL et al.: Intracellular CXCR4+ cell targeting with T22-empowered protein-only nanoparticles. Int J Nanomedicine 2012, 7: 4533-4544.

Unzueta U, Saccardo P, Domingo-Espin J, Cedano J, Conchillo-Sole O, Garcia-Fruitos E et al.: Sheltering DNA in self-organizing, protein-only nano-shells as artificial viruses for gene delivery. Nanomedicine 2014, 10: 535-541.

Van DS, Bronselaer A, Nielandt J, Stalmans S, Wynendaele E, Audenaert K et al.: Brainpeps: the blood-brain barrier peptide database. Brain Struct Funct 2012, 217: 687-718.

Vazquez E, Roldan M, Diez-Gil C, Unzueta U, Domingo-Espin J, Cedano J et al.: Protein nanodisk assembling and intracellular trafficking powered by an arginine-rich (R9) peptide. Nanomedicine (Lond) 2010, 5: 259-268.

Vazquez E, Villaverde A: Microbial biofabrication for nanomedicine: biomaterials, nanoparticles and beyond. Nanomedicine (Lond) 2013, 8: 1895-1898.

Vazquez E, Ferrer-Miralles N, Villaverde A: Peptide-assisted traffic engineering for nonviral gene therapy. Drug Discov Today 2008, 13: 1067-1074.

Wagner S, Zensi A, Wien SL, Tschickardt SE, Maier W, Vogel T et al.: Uptake Mechanism of ApoE-Modified Nanoparticles on Brain Capillary Endothelial Cells as a Blood-Brain Barrier Model. 2012, 7.